International Journal of Science Academic Research
Vol. 04, Issue 11, pp.6653-6657, November, 2023
Available online at http://www.scienceijsar.com

ISSN: 2582-6425

Research Article

EFFECT OF THE $MoSe_2$ LAYER AT THE ABSORBER/REAR CONTACT INTERFACE ON THE PERFORMANCE OF THE CIGS SOLAR CELL

***Boureima Traoré, Soumaïla Ouedraogo, Adama Zongo, Issiaka Sankara, Marcel Bawindsom Kébré, Daouda Oubda and Francois Zougmoré**

Département de Physique, Laboratoire de Matériaux et Environnement (LA.M.E)-UFR/SEA, Université Joseph Ki-ZERBO, 03 BP 7021 Ouagadougou 03, Burkina Faso

Received 27th September 2023; **Accepted** 24th October 2023; **Published online** 30th November 2023

Abstract

In this article, based on numerical simulation, SCAPS-1D software was used to investigate the influence of the$MoSe_2$ layer at the CIGS/Mo interface on the performance of the CIGS solar cell. Analysis of the effect of the thickness and bandgap width of the $MoSe_2$ layer revealed that optimum performance is obtained with a $MoSe_2$ layer of 0.030 µm thickness and a bandgap of 1.3 eV. Subsequently, the J-V characteristic and quantum efficiency of the CIGS solar cell with optimal layer parameters $MoSe_2$ were compared with the cell without $MoSe_2$. This analysis demonstrated that the presence of this optimized $MoSe_2$ layer at the CIGS/Mo interface improves the electrical performance of the solar cell.

Keywords: CIGS solar cell, Numerical simulation, $MoSe_2$ thickness, $MoSe_2$ band gap, SCAPS-1D software, CIGS/Mo interface.

INTRODUCTION

In the field of photovoltaic solar cells, CIGS-based thin-film solar cells occupy a prominent position due to their low production cost and excellent conversion efficiency reaching 23.35% published in 2019 by [15]**.** This record efficiency can be linked to the quality of the interface between the CIGS absorber and the molybdenum back contact. The CIGS/Mo interface is a high recombination zone, particularly for ultrathin absorbers [1]**.** In CIGS-based thin-film solar cells, the main role of the CIGS absorber is to form the P-N hetero junction with the CdS buffer layer and more efficiently convert incident photons into electron-hole pairs [3]**.** The role of the back contact is to provide a positive electrical contact to collect photo generated holes resulting from the absorption of incident light photons [8]**.** The permeability of the back contact allows selenium (Se) atoms to react with molybdenum (Mo) during the CIGS deposition process to form a thin layer of $MoSe_2$. The formation of the $MoSe_2$ layer can be attributed to several factors, such as the pressure during molybdenum sputtering [12][13]**,** the concentration of sodium present in the soda-lime glass that diffuses into the CIGS absorber[11][25][26], as well as the selenization temperature[1]**.** Numerous studies concur that the $MoSe_2$ layer contributes to improved adhesion between molybdenum (Mo) and the glass substrate [10][25]. Furthermore, the $MoSe_2$ layer at the CIGS/Mo interface has a beneficial effect by transforming the CIGS/Mo hetero-contact from a Schottky-type into an ohmic-type contact [10][21][24]**.** Can the presence of the $MoSe_2$ layer at the back interface significantly impact the performance of the solar cell CIGS? In this article, we will determine the optimal parameters for the $MoSe_2$ layer to achieve high-efficiency CIGS solar cells. Initially, we will investigate the influence of the thickness and bandgap of the $MoSe_2$ layer on the CIGS solar cell's performance to determine the optimal values. Subsequently, a comparative study of the J-V characteristic and quantum efficiency of the CIGS solar cell with and without the $MoSe_2$ layer will be conducted.

Corresponding Author:** ***Boureima Traoré,
Département de Physique, Laboratoire de Matériaux et Environnement (LA.M.E)-UFR/SEA, Université Joseph Ki-ZERBO, 03 BP 7021 Ouagadougou 03, Burkina Faso

MATERIALS AND METHODS

Numerical simulation is a technique that involves using a computer to model and replicate the behavior of a solar cell without conducting the actual experiment. It allows for the characterization of photovoltaic solar devices. In this study, we intend to utilize the SCAPS-1D software [16] to perform our numerical simulations. The SCAPS-1D software employs the finite difference method with well-defined boundary conditions to solve the fundamental equations, which include the Poisson equation and the continuity equations for electrons and holes [17].Thin-film solar cells based on CIGS are hetero junction solar cells in which the p-type CIGS serves as the absorber of the cell. The CIGS absorber is the most crucial layer of the device and occupies the majority of the solar cell's surface [7] [22].On this absorber, an n-type CdS buffer layer is used to create the P-N junction. A high-resistivity transparent conductive oxide (TCO) layer is deposited onto the buffer layer. The entire assembly is placed on a substrate, which serves as the mechanical support. Typically, soda-lime glass is the most commonly used substrate in high-efficiency CIGS solar cells due to its compatibility with the CIGS absorber[2][23].The front contacts (Ni/Al) and back contact (Mo) are added to collect the photo-generated electrons and holes. The structure of such a solar cell is shown in Figure 1a.

In the CIGS solar cell, the permeability of molybdenum allows selenium atoms from the absorber to diffuse. This diffusion of selenium from the absorber will give rise to a thin layer of molybdenum diselenuire$MoSe_2$ in very small amounts after annealing at 600 °C [2][19]. The structure of the solar cell with the $MoSe_2$ layer is shown in figure 1.b. The presence of the $MoSe_2$ layer at the CIGS/Mo interface is also highlighted by transmission electron microscope (TEM) and scanning electron microscope (SEM) images[13] as shown in Figure 2.

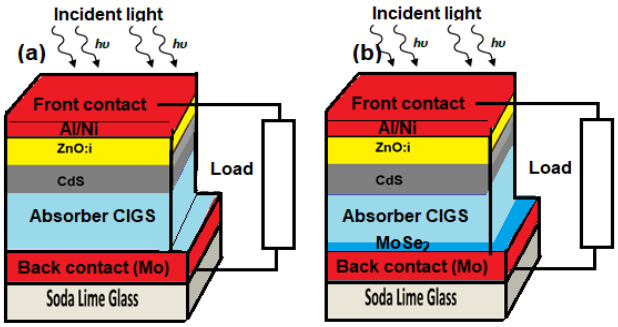

Figure 1. Solar cell structure without the $MoSe_2$ layer (a) and with the $MoSe_2$ layer (b) used for numerical simulation.

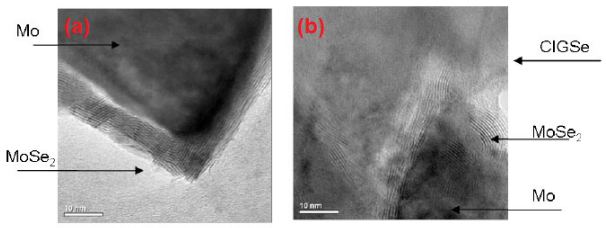

Figure 2. CIGS/Mo interface observed by TEM and SEM [13]

Table 1:Properties of the$MoSe_2$ layerused for simulation

Layersproperties	$MoSe_2$ layer
Thickness (nm)	variable
Band gap (eV)	variable
Electron Affinity (eV)	4.372
Diélectric relative Permittivity	13.6
Effective densité of state in BC (cm^{-3})	$2.2 * 10^{18}$
Effective densité of state in BV (cm^{-3})	$1.8 * 10^{19}$
Electrons thermal velocity (cm/s)	10^7
Holes thermal velocity (cm/s)	10^7
Electrons Mobility (cm^2/Vs)	100
HolesMobility (cm^2/Vs)	25
Doping concentration (cm^{-3})	10^{16}

The equivalent band diagram of the CIGS solar cell with the $MoSe_2$ layer is shown in figure 3.

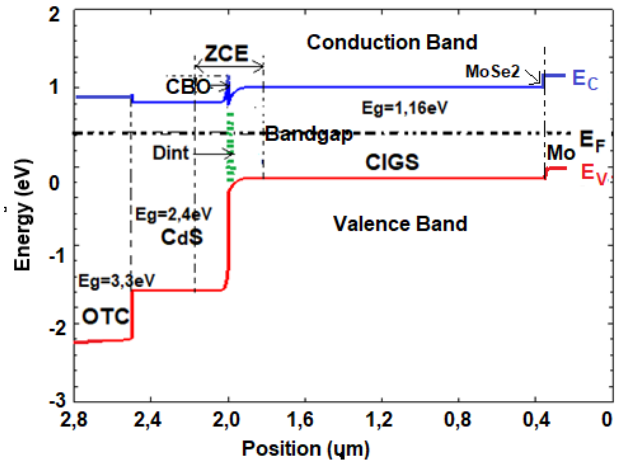

Figure 3. Energy band diagram with $MoSe_2$ layer

The properties of the $MoSe_2$ layer are summarized in Table 1 and the properties of the various layers used for the numerical simulation are summarized in Table 2. These properties were obtained from theoretical and experimental results [6][18][20]. The solar cell temperature is maintained at 300K. It is illuminated under standard conditions by an AM 1.5G spectrum that takes direct and diffuse radiation into account [5].

Table 2. The solar cell simulation parameters used in SCAPS-1D

Layers properties	i-Zno	CdS	CIGS
Thickness (nm)	300	50	2500
Band gap (eV)	3,3	2,4	1,25
Electron Affinity (eV)	4,55	4,45	4.5
Diélectric relative Permittivity	9,00	10	13,6
Effective density of state in BC (cm^{-3})	$3,1.10^{18}$	$3,1.10^{18}$	$2,10^{18}$
Effective density of state in BV (cm^{-3})	$1,8.10^{19}$	$3,1.10^{18}$	$1,5.10^{19}$
Electrons thermal velocity (cm/s)	$2,4.10^7$	$2,4.10^7$	$3,9.10^7$
Holes thermal velocity (cm/s)	$1,3.10^7$	$1,6.10^7$	$1,4.10^7$
Electrons Mobility (cm^2/Vs)	100	72	100
Holes Mobility (cm^2/Vs)	31	20	12.5
Doping concentration (cm^{-3})	10^{17} (D)	10^{17} (D)	10^{16} (A)

To validate our results, we compared the J-V characteristic curves of our numerical simulation with those obtained experimentally by Pettersson. We can see that there is good agreement between these two results, as shown in Fig. 4, which leads us on to the results and discussion chapter.

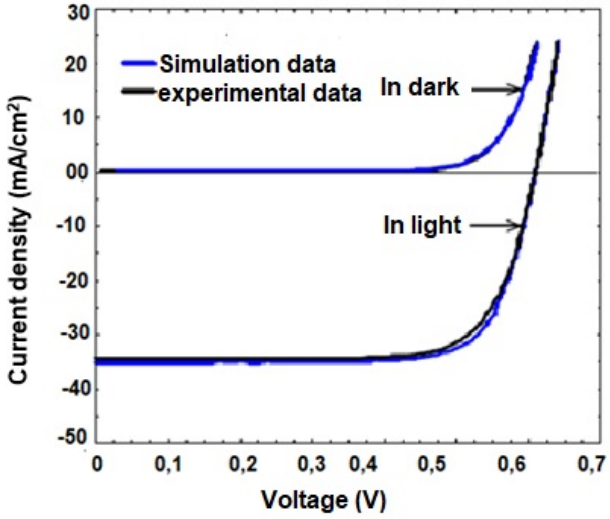

Figure 4. Curves J-V characteristics compared with experimental of d Pettersson *et al.* [20]

Materials and methodology

Effect of the thickness of $MoSe_2$ layer

The CIGS/Mo interface is a high recombination zone, especially for ultrathin absorbers. The $MoSe_2$ layer with its 1.4 eV bandgap could serve as an effective electron reflector, crucial for reducing recombination at the CIGS/Mo interface [1][3]. However, an optimal thickness of the $MoSe_2$ layer is necessary, because a very thick $MoSe_2$ layer limits current collection capacity at the back electrode due to the high resistivity of $MoSe_2$ (10^1- $10^4\Omega$.cm) et thus deteriorating electrical parameters [4] [14]. Therefore, optimizing the thickness of the $MoSe_2$ layer is essential to fulfill its role as an electron reflector at the back interface. To elucidate the benefits of the $MoSe_2$ layer, we conducted numerical simulations, focusing solely on its thickness, which appears to be the critical parameter at the CIGS/Mo interface. The thickness of the $MoSe_2$ layer is limited to a few tens of nanometers below 500 °C and increases beyond 550 °C [1]. To

perform this numerical simulation, we varied the thickness of the $MoSe_2$ layer from 0.005 µm to 0.05 µm. Figure 5 illustrates the influence of the $MoSe_2$ layer thickness on the J-V characteristic and quantum efficiency. From these results, we observe that increasing the thickness of the $MoSe_2$ layer has a slight impact on the J-V characteristic, as shown in Figure 5.a. The same trend is observed for the quantum efficiency in figure5.b, resulting in almost complete absorption of incident photons when the $MoSe_2$ layer thickness ranges from 0.005 µm to 0.05 µm.

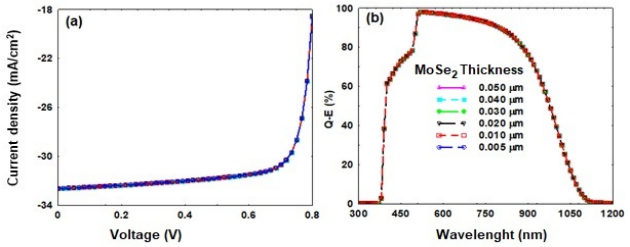

Figure 5. J-V characteristics (a) and quantum efficiency Q-E (b) for different thicknesses of $MoSe_2$ layer

For further explanation, we will extract the electrical parameters from the J-V characteristic. These electrical parameters are summarized in Table 2**.**

Table 2. Electrical parameters for different thickness of $MoSe_2$ layer

Thickness of $MoSe_2(\mu m)$	η (%)	FF (%)	J_{SC} (mA/cm^2)	V_{OC} (V)
0.005	21,8189	78,0428	32,6239	0,857
0.01	21,8214	78,0358	32,625	0,8571
0.02	21,824	78,0292	32,6265	0.8572
0.03	21,8248	78,0276	32,6272	0,8573
0.04	21,8249	78,028	32,6274	0,8573
0.05	21,8250	78,0292	32,6275	0,8573

In this table, we see a very slight increase in theconversion efficiency η, open-circuit voltage V_{OC} and short-circuit current density J_{SC} as the thickness of the $MoSe_2$ increases. This slight increase in these various electrical parameters may be due to a slight absorption of incident photons as the thickness of the $MoSe_2$ increases. It should be remembered that increasing the thickness of the $MoSe_2$ layer affects solar cell performance.

Effect of the band gap of $MoSe_2$layer

To carry out the numerical simulation in this section, we vary the thickness of the $MoSe_2$ layer from 1.0 eV to 1.4 eV by setting the thickness of the $MoSe_2$layer at 50 nm. Figure 6shows the influence of the bandgap of the $MoSe_2$layer on the J-V characteristc and quantum efficiency. We find that increasing the bandgap of the $MoSe_2$layer slightly influences the J-V characteristic (figure 7.a) and the quantum efficiency (Figure 6.a).

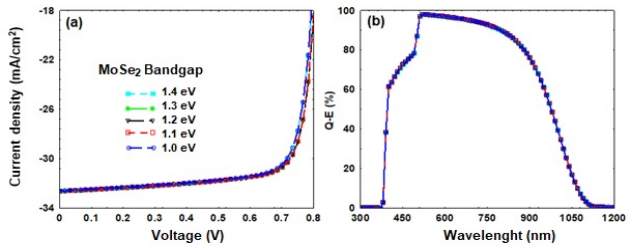

Figure 6, J-V characteristics (a) and quantum efficiency Q-E (b) for different bandgap of $MoSe_2$ layer

To understand the J-V characteristic curves, we'll extract the electrical parameters, which are summarized in table3**.**

Table 3. Electrical parameters for different bandgap of $MoSe_2$ layer

Bandgap of $MoSe_2(\mu m)$	η (%)	FF (%)	J_{SC} (mA/cm^2)	V_{OC} (V)
1	21,5091	78,4168	32,5975	0,84145
1,1	21,8034	78,0268	32,6195	0,85665
1,2	21,8214	78,0358	32,6251	0,8571
1,3	21,8146	78,0612	32,625	0,8565
1,4	21,5187	78,415	32,6139	0,8414

When the bandgap is less than 1.30 eV (Eg<1.30 eV), there is a slight increase in efficiency η, open-circuit voltage V_{OC} and short-circuit current density V_{OC}, as shown in Table 3. Above this value, a slight decrease in all electrics is observed. It should be noted that the increase in the bandgap of the $MoSe_2$ layer influences the performance of the solar cell slightly.

Simultaneous influence of thickness and bandgap of the $MoSe_2$ layer

In this part of the work, we will simultaneously study the influence of $MoSe_2$ thickness and bandgap on cell performance in order to determine the optimal electrical parameters as shown in Figure 7.

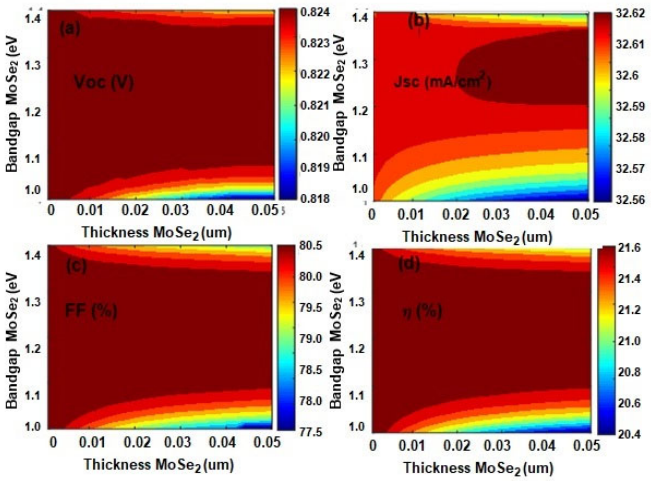

Figure 7. Influence of bandgap on electrical parameters for different thicknesses of $MoSe_2$

The studies carried out in the previous sections have shown that the thickness and bandgap of the $MoSe_2$ layer are parameters that slightly influence the performance of the CIGS solar cell. When the thickness of the $MoSe_2$ layer is very small, i.e. less than 0.005 µm, very good performance is achieved with whatever the bandgap of the $MoSe_2$ layer. Beyond 0.005 µm, all the electrical parameters of the solar cell decrease when the bandgap of the $MoSe_2$ layer is below 1.1 eV and above 1, 35 eV. Au-Above 0.005 µm, very good performances are obtained when the band gap of the $MoSe_2$ layer is between 1.1 eV and 1.35 eV. Optimum short-circuit current density values are obtained for a bandgap between 1.25 eV and 1.35 eV and a layer thickness $MoSe_2$ greater than 0.020 µm. It can be concluded that very good performance is achieved with a $MoSe_2$ layer thickness of 0.030 µm and a bandgap between 1.25 eV and 1.35 eV.

Comparative study of cell performance with and without the $MoSe_2$ layer

In this work, we will make a comparative study of the J-V characteristic and quantum efficiency of solar cell performance with and without the $MoSe_2$ layer. For this study, the thickness of the $MoSe_2$ layer is fixed at 0.030 µm and its band gap is set at 1.3 eV. The J-V characteristic and Q-E quantum efficiency curves are shown in Figure 8.

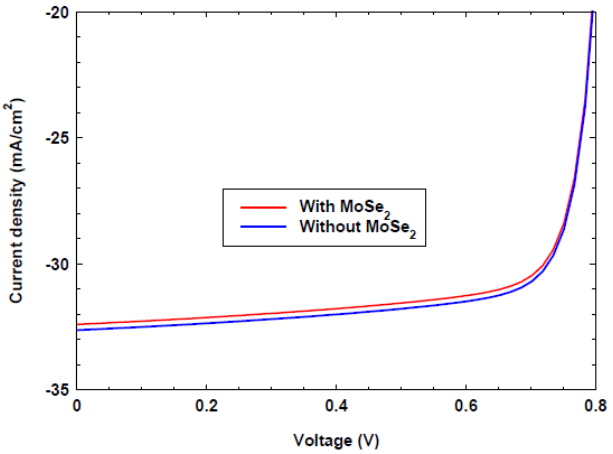

Figure 8. J-V characteristics of cell performance without $MoSe_2$ and with $MoSe_2$

From the J-V characteristic curve, we extracted the electrical parameters of the solar cell. These parameters are summarized in table 4.

Table 4. Electrical parameters of the solar cell without $MoSe_2$ and with $MoSe_2$

	V_{OC} (V)	J_{SC} (mA/cm^2)	FF (%)	η (%)
Without $MoSe_2$	0.854410	32.39950738	78.1941	21.64
With $MoSe_2$	0.856938	32.63002626	78.0145	21.82

In the presence of the $MoSe_2$ layer, we see that the conversion efficiency of the solar cell increases from 21.6460% to 21.8143%, ie. a gain in conversion efficiency Δη = 0.18%. The same applies to open-circuit voltage V_{OC} and short-circuit current density J_{SC} with gains ΔV_{OC}=0.00253V and ΔJ_{SC}=0.2305 mA/cm^2respectively.

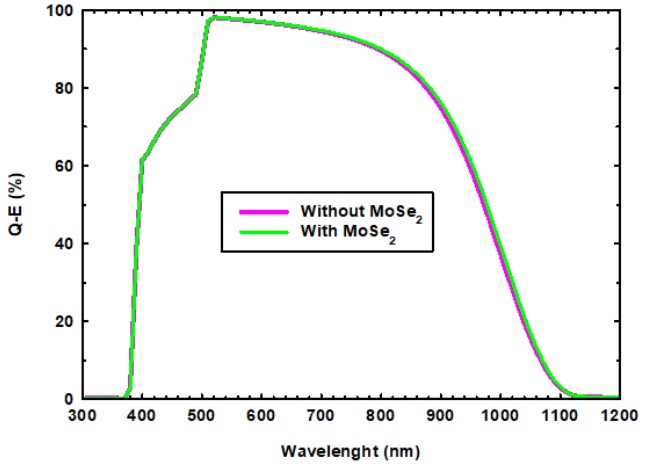

Figure 9. Q-E quantum efficiency of cell performance without $MoSe_2$ and with $MoSe_2$

The open-circuit voltage V_{OC} increases due to the passivation of defects of the CIGS/Mo interface as in the case of the Al_2O_3layer [9]. This increase in electrical parameters can be explained by the presence of the $MoSe_2$ layer at the CIGS/Mo back interface. It can also be explained by the increased absorption of incident photons into electron-hole pairs when the wavelength exceeds 800 nm as shown in Figure 9. For shorter wavelengths of light photons, there is no absorption, as shown in Figure 9.This performance can be explained by the reduced interactions between the holes collected at the back contact and the electrons photogenerated in the absorber CIGS. Indeed, the $MoSe_2$ layer can be seen as an electron reflector at the back interface, thus helping to reduce back interface charge carrier recombination hence improving CIGS solar cell performance.

Conclusion

At the end of this study on the CIGS/Mo interface, it emerges that the variation in the thickness of the $MoSe_2$ layer as well as its band gap have an influence on the performance of CIGS solar cells. Simulation results show that very good performance is achieved with a $MoSe_2$ layer of 0.030 µm thickness and a bandgap of 1.3 eV. A comparison of the electrical performance of the solar cell with its optimal $MoSe_2$ layer parameters with that of a CIGS cell without $MoSe_2$ shows that the performance of the solar cell with a $MoSe_2$ layer is better. This study constitutes a serious avenue for developing high-efficiency CIGS solar cells by optimizing the deposition process so as to obtain a thin $MoSe_2$ layer at the CIGS/Mo interface.

REFERENCES

1. Abou-Ras, D., Kostorz, G., Bremaud, D., Kelin, M., Kurdesau, F.V., Tiwari, A.N., &Debeli, M. 2005. Formation and characterisation of $MoSe_2$ for $CuInGaSe_2$ based solar cells. *Thin Solid Films,* 480481 (2005) 433 438, 480481 (2005), 433 438.
2. Buffière, M. 2011. Synthèse et caractérisation de couches minces de Zn(O,S) pour application au sein des cellules solaires à base de $CuInGaSe_2$. Ph.D. thesis, Université de Nantes.
3. Duchatelet, A. 2012. Synthèse de couches minces de Cu(In, Ga)Se2 pour cellules solaires par électrodépôt d'oxydes mixtes de cuivre-indium-gallium. Ph.D. thesis, Université Lille1.
4. Cozza, D., Ruiz, C. M., Duche, D., Simon, J. J. et Escoubas, L. (2016). Modeling the back contact of $Cu_2ZnSnSe_4$solar cells. IEEE Journal of Photovoltaics, 6:1296.
5. Fabre, W. 2011. Silicim de type pour cellules solaires à hétérojonction : caractérisations et modélisations. Ph.D. thesis, Université de paris-sud 11.
6. Gloeckler, M. 2005. Device physics of thin-film solar cells. Ph.D. thesis, Colorado State University.
7. Gloeckler, M., & Sites, J.R. 2005. Efficiency Limitations for Wide-Band-Gap Chalcopyrite Solar Cells. Thin Solid Films 480 (2005) 241-245, 480, 241–245.
8. Kanevce, A. 2007. Anticipated performance of $Cu(In, Ga)Se_2$solar cells in the thin film limit. Ph.D. thesis, Colorado State University.
9. Klinkert, T., Theys, B., Patriarche, G., Jubault, M., Donsanti, F., Guillemoles, J. F. et Lincot, D. (2016). New

insights into the $Cu(In,Ga)Se_2$/Mo interface in thin film solar cells : Formation and properties of the mose2 interfacial layer. *J. Chem. Phys,* 145:154702.

10. Kohara, N., Nishiwaki, S., Hashimoto, Y., Negami, T. et Wada, T. (2001). Electrical properties of the $Cu(In,Ga)Se_2$ / $MoSe_2$/Mo structure. *Solar Energy Materials and Solar Cells,* 67:209–215.
11. Lin, Y. C., Shen, M. T., Chen, Y. L., Hsu, H. R. et Wu, C. H. (2014). A study on $MoSe_2$ layer of Mo contact in $Cu(In,Ga)Se_2$ thin film solar cells. *Thin Solid Films,* 570:166U171.
12. Lin, Y. C., Hong, D. H., Hsieh, Y. T., Wang, L. C. et Hsu, H. R. (2016). Role of mo :na layer on the formation of $MoSe_2$ phase in $Cu(In,Ga)Se_2$ thin film solar cells. Solar Energy Materials and Solar Cells, 155:226U233.
13. Matthieu. T., Synthèse de couches minces de molybdène et application au sein des cellules solaires à base de $Cu(In,Ga)Se_2$ co-évaporé 2013.
14. Minbashi, M., Omrani, M. K., Melarian, N. et Kim, D. H. (2017). Comparison of theoretical and experimental results for band-gap-graded CZTSe solar cell. Current Applied Physics, 17:1238–1243.
15. Nakamura, M., Yamaguchi, K., Kimoto, Y., Yasaki, Y.,Kato, T., & Sugimoto, H. (2019). Cd-free Cu (In,Ga)(Se,S)2 thin-film solar cell with record efficiency of 23.35%. IEEE Journal of Photovoltaics, 9(6), 1863-1867.
16. Niemegeers, A., Burgelman, M., Herberholz, R., Rau, U., Hariskos, D., & Schock, H.-W. 1998. Model for electronic transport in $Cu(In,Ga)Se_2$ Solar Cells. Applied Physics Letters, 6, 407-421.
17. Niemergeers, A., &Burgelman, M. 1997. Effects of the Au/CdTe back contact on IV and CV characteristics of Au/CdTe/CdS/TCO solar cells. *J. Appl. Phys.,* 81, No. 6, 2881–2886.
18. Ouédraogo, S., Zougmoré, F., &Ndjaka, J. M. B. (2014). Computational analysis of the effect of the surface defect layer (SDL) properties on $Cu(In,Ga)Se_2$ based solar cell performances. *Journal of Physics and Chemistry of Solids,* 75(5), 688-695.
19. Painchaud, T., 2010. Mécanismes de croissance des couches minces de $Cu(In,Ga)Se_2$ coévaporées : vers des synthèses rapides et à basse température. Ph.D. thesis, Université de Nantes.
20. Pettersson, J., Platzer-Björkman, C., Zimmermann, U., & Edo_, M. 2011. Baseline model of graded-absorber Cu(In;Ga)Se_2 solar cells applied to cells with $Zn_{1-x}Mg_xO$ buffer layers. *Thin Solid Films,* 519, 7476–7480.
21. Pouzet, J. et Bernede, J. C. (1990). $MoSe_2$ thin film synthesized by solid state reactions between Mo and Se thin films. Rev. Phys. Appl., 25:8007.
22. Ribeaucourt, L. 2011. Electrodépôt et sélénisation d'alliages Cu-In-Ga en vue de la synthèse de couches minces de Cu(In,Ga)Se_2 pour cellules solaires. Ph.D. thesis, Université Pierre et Marie Curie.
23. Shin, Y. M., Shin, D.H., Kim, J. H., & Ahn, B.T. 2011. Effect of Na doping using Na_2S on the structure and photovoltaic properties of CIGS solar cells. *Current Applied Physics,* 11, S59–S64.
24. Rostan, P. J., Mattheis, J., Bilger, G., Rau, U. et Werner, J. (2005). Formation of transparent and ohmic ZnO:Al / $MoSe_2$ contacts for bifacial $Cu(In,Ga)Se_2$ solar cells and tandem structures. *Thin Solid Films,* 480-481:67–70.
25. Wada, T., Kohara, N., Nishiwaki, S. et Negami, T. (2001). Characterization of the $Cu(In,Ga)Se_2$ /Mo interface in CIGS solar cells. *Thin Solid Films 387*, 387:118–122.
26. Wurz, R., Marron, D. F., Meeder, A., Rumberg, A., Babu, S., Niedrig, T. S., Bloeck, U., Bischoff, P. S. et Steiner, M. C. L. (2003). Formation of an interfacial $MoSe_2$ layer in CVD grown $CuGaSe_2$ based thin film solar cells. *Thin Solid Films*, 431-432:398.

****